Landslides (2014) 11:425–439
DOI 10.1007/s10346-013-0391-7
Received: 8 May 2012
Accepted: 11 February 2013
Published online: 28 February 2013

Taskin Kavzoglu · Emrehan Kutlug Sahin · Ismail Colkesen

Landslide susceptibility mapping using GIS-based multi-criteria decision analysis, support vector machines, and logistic regression

Abstract Identification of landslides and production of landslide susceptibility maps are crucial steps that can help planners, local administrations, and decision makers in disaster planning. Accuracy of the landslide susceptibility maps is important for reducing the losses of life and property. Models used for landslide susceptibility mapping require a combination of various factors describing features of the terrain and meteorological conditions. Many algorithms have been developed and applied in the literature to increase the accuracy of landslide susceptibility maps. In recent years, geographic information system-based multi-criteria decision analyses (MCDA) and support vector regression (SVR) have been successfully applied in the production of landslide susceptibility maps. In this study, the MCDA and SVR methods were employed to assess the shallow landslide susceptibility of Trabzon province (NE Turkey) using lithology, slope, land cover, aspect, topographic wetness index, drainage density, slope length, elevation, and distance to road as input data. Performances of the methods were compared with that of widely used logistic regression model using ROC and success rate curves. Results showed that the MCDA and SVR outperformed the conventional logistic regression method in the mapping of shallow landslides. Therefore, multi-criteria decision method and support vector regression were employed to determine potential landslide zones in the study area.

Keywords Landslide · Susceptibility mapping · Multi-criteria decision analysis · Support vector machine · Logistic regression

Introduction

A natural disaster is the effect of an unexpected change in environmental conditions (e.g., earthquake, tsunami, flood) which causes significant level of financial, environmental, or human losses. Landslides, one of the most destructive natural disasters, produce drastic changes in the morphology of the landscape and damages to natural and artificial structures on the Earth. Landslides are described as mass movements of soil or rock that involve shear displacement along one or several slip surfaces, which are either visible or may be reasonably inferred (Varnes 1978). Determining landslide-prone areas is important to ensure the safety of human life and avoid negative impacts on the regional and national economy. Determination of landslide-susceptible zones, producing accurate and up-to-date landslide susceptibility maps have been highly studied research topics in hazard management. These maps provide valuable information for government agencies, planners, decision makers, and local landowners to make emergency plans to reduce the negative effects on infrastructure, superstructure, and human life.

The physical characteristics of Turkey, including tectonic activities, geological structure, topographical, and meteorological features, frequently cause natural hazards resulting in social–economic and life losses of great consequence in the region. Turkey has recently experienced several natural disasters, which resulted in great loss of human life, injuries, and property damages. When natural disasters were ordered in terms of their occurrences, landslides take the second place after the earthquakes. Landslides, particularly shallow ones, are mostly experienced in Black Sea, Central, and Eastern Anatolian regions. In Turkey, the highest number of landslides has been recorded in the province of Trabzon. Since 1929, many people have lost their lives in this region (Ergünay 2007; Bayrak and Ulukavak 2009).

Up to now, many techniques have been developed and applied in the literature to produce landslide susceptibility maps. Landslide modeling techniques can be grouped into several broad categories, namely geomorphological hazard mapping, analysis of landslide inventories, heuristic methods, and statistical or geotechnical models (Guzzetti et al. 1999). Within these techniques, probabilistic and statistical methods have been widely used to determine landslide susceptibility zones. Among the most popular and widely used statistical method is the logistic regression that has been applied in many local- and regional-scale landslide susceptibility modeling (Dai et al. 2001; Ayalew and Yamagishi 2005; Bai et al. 2011; Devkota et al. 2013). Recently, geographical information system-based multi-criteria decision analysis has been used to carry out landslide susceptibility assessment (Castellanos Abella and Van Westen 2007; Armas 2011; Akgun 2012; Neuhauser et al. 2012). Geographic information system (GIS)-based multi criteria decision analysis (MCDA) can be defined as a decision aid and a mathematical tool allowing the comparison of different alternatives or scenarios according to many criteria, often conflicting, in order to guide the decision maker toward a judicious choice (Roy 1996). Lately, non-parametric techniques including artificial neural networks, decision trees, and support vector machines have been also employed for susceptibility mapping. Specifically, support vector machines (SVMs), introduced as a robust data mining approach, have been applied to both classification and regression problems including landslide susceptibility mapping (Yao et al. 2008; Fu and He 2010; Yilmaz 2010; Pradhan 2013).

In this study, the MCDA, support vector machine regression (SVR), and logistic regression methods were used to produce a landslide susceptibility map of Trabzon province where shallow landslides are particularly recurrent. Performances of the MCDA and SVR methods were compared with the performance of logistic regression method that was regarded as benchmark method in this study. Landslide inventory map of the study area, formed through field observations, was used to estimate the accuracies of the landslide susceptibility maps. In addition to the evaluations on performances using standard accuracy measures (i.e., user's and overall accuracies), receiver operating characteristics (ROC), and success rate curves were applied to make objective and sound comparisons between the methods.

Study area and data

The study area is the Trabzon province, a 4,664-km^2 area located south of the Black Sea (NE Turkey). It is situated between 39°15′ and 40°15′ longitudes and 41°8′ and 40°30′ latitudes. The climate is characteristic of the Black Sea region with temperate in summers and raining season normally lasting from September to April. The annual average amount of rain falls in the province is about 830 mm. Nevertheless, the rainfall regime is irregular, with some periods of rare precipitation with long-lasting heavy rains. In the region, the rough topography, susceptible weathering units, and the temperate climate means that many new landslides appear from time to time, as a result of heavy rainfalls (Yalcin et al. 2011). Heavy rainfall and dense vegetation have increased the speed of weathering which then considerably reduced the resistance of the overlying units to the risk of landslides (Yalcin 2011).

Geological units of the study area are mainly represented by Secondary and Tertiary eras consisting of Lias-Dogger (Jlh), Upper Jurassic–Lower Cretaceous (JCr), Upper Cretaceous–Paleocene (Cru1, Cru2, Cru3, Cru4b, Cru5b, Cru5a), Eocene (γ_2, γ_3, Ev), and Pliocene (Pl) epochs. These rocks are overlain by alluvium, the youngest unit, which is Quaternary aged. Due to the highly saturated loamy formation and continuous exposure to heavy rain, shallow landslide occurrence has consistently increased. Another considerable effect on the increase of landsliding is the steep slope that begins just from the shore. Although natural causes are considered as major contributing factors, human factors such as infrastructure, superstructure, and deforestation also play an important role in the initiation of shallow landslides in Trabzon province.

Landslide inventory map

Shallow landslide occurred lands were defined as vector polygons using handheld Global Positioning System equipment whilst non-landslide fields, which were required for learning processes, were determined by applying the approach proposed by Gómez and Kavzoglu (2005). These polygons were later converted to raster data that were in 30 m resolution. The approach is based on two basic facts: Landslide activity is not likely to happen on river channels and on terrains with slope angles lower than 5°. As a result of above considerations, 12,029 pixels representing landslide occurrence and 6,280 pixels representing landslide safe areas (i.e., non-landslide zones) were determined. All pixels were combined into a single image forming the ground reference map (Fig. 1).

In this study, nine thematic maps associated with lithology, slope, aspect, land cover, drainage density, topographic wetness index, elevation, slope length, and distance to road were utilized for landslide susceptibility mapping. These images were registered to the Universal Transverse Mercator projection system using ArcGIS software package. Registered images were stacked on to each other to form a multi-layer image that was utilized in further stages.

Estimation of input parameters

Landslide susceptibility mapping requires evaluating a number of land-related factors together. Studies in the literature consider a variety of parameters including lithology, slope, aspect, elevation, curvature, land use/cover types, and drainage density (Dai and Lee 2002; Ayalew et al. 2004; Brenning 2005). Moreover, several studies have regarded additional parameters such as lineaments, topographic wetness index (TWI), distance to road or settlements, normalized difference vegetation index, and soil types for susceptibility mapping (Gómez and Kavzoglu 2005; Yilmaz 2010; Pradhan and Lee 2010). In addition to these parameters, soil thickness and meteorological conditions that can be considered as a triggering factor and pre-failure conditions of the recent landslides can be considered in landslide modeling studies (Santacana et al. 2003; Suzen and Doyuran 2004; Segoni et al. 2012). In this study, lithology, slope, land cover, aspect, elevation, drainage density, slope length, topographic wetness index, and distance to road were considered as major factors to produce landslide susceptibility map of the study area.

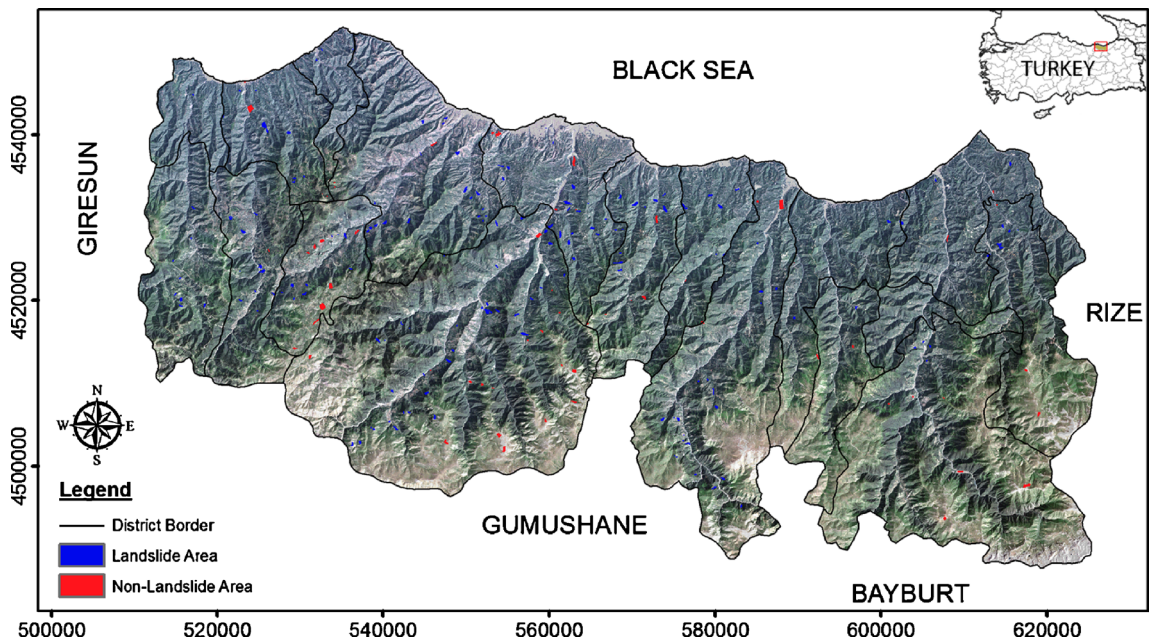

Fig. 1 Ground reference map containing landslide and non-landslide area

Slope

Slope angle is one of the most important factors controlling the stability of slopes. Slope angle is the form between any part of the surface of the earth and a horizontal datum. Most of the studies in literature underline that slope is a major factor causing landslides (Dai and Lee 2002; Ayalew et al. 2004; Gómez and Kavzoglu 2005). In order to obtain a slope angle map, digital elevation model (DEM), produced from 1:25.000-scale topographic maps, was utilized. The resulting thematic map showed that slope angles ranged from 0° to 86° in the study area. About 33 % of the study area consists of slopes at 0–20° interval, whilst the rest has higher slopes. Indicating the mountainous characteristic of the region, this finding was the driving force for the inclusion of slope factor in determining landslide-prone areas in the study area. The slope map of the study area was categorized into 5° intervals, and thus eight subclasses (0–5, 5–10, 10–15, 15–20, 20–25, 25–30, 30–35, 35–86) were formed. As suggested by many researchers (e.g., Nandi and Shakoor 2010; Yalcin et al. 2011), equal intervals were applied to determine subclasses.

Lithology

Lithology is one of the main factors having a direct effect on the occurrence of landslides since lithological and structural variations often lead to changes in strength and permeability of rocks and soils. Therefore, many researches have considered lithology as an input parameter to determine landslide susceptibility (Dai and Lee 2002; Ayalew et al. 2005; Wang et al. 2009). The geological map of the study area, including 13 lithological units (Fig. 2), was created from 1:100,000-scale geological map published by the General Directorate of Mineral Research and Exploration of Turkey in 1998 (www.mta.gov.tr).

Each lithological unit was weighted considering both studies in the literature and a frequency analysis applied to the landslide inventory map. The analysis revealed that landslides mainly occurred in Ev and upper Cretaceous units (Cru1, Cru2, Cru3, and Cru4b) to which high weights were assigned. These units mainly comprise basalt, andesite, pyroclastics, and intercalations of sandstones clayey limestone and siltstones. It should be noted that this preliminary finding is parallel to the results given by Yalcin (2011).

Land cover

Land cover is one of the most sensitive parameters easily affected by the changes from the environment and human activities. Therefore, land cover structure of a region inspires the planning scenarios in landslide management. Some researches (e.g., Restrepo et al. 2003; Begueria 2006) have underlined the importance of land cover in slope instability processes and in landslide hazard assessments. Vegetation types are affected by soil hydrology during increased rainfall interception, infiltration, and

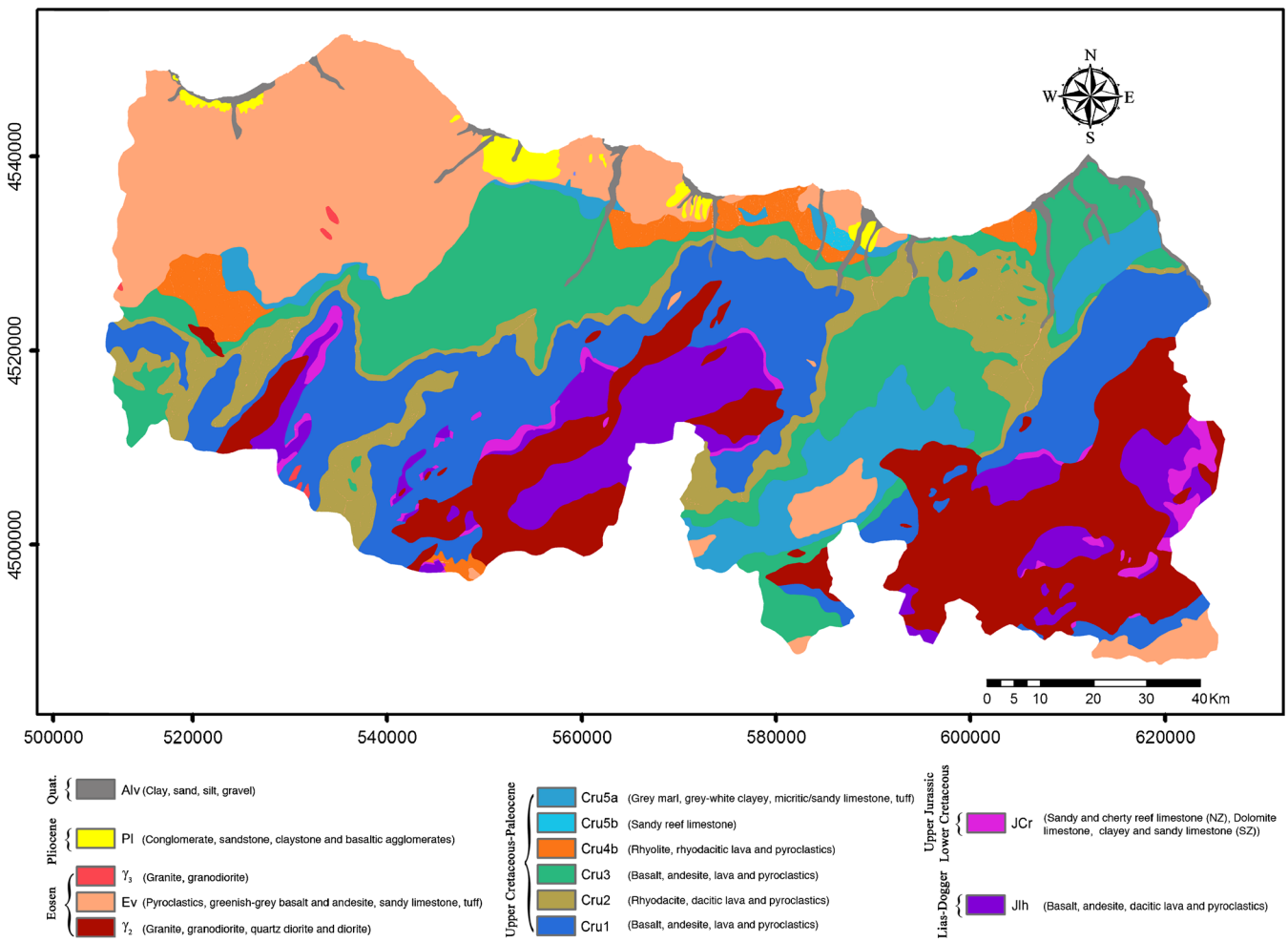

Fig. 2 Lithological map of the study area

evapotranspiration. Interception and evapotranspiration contribute on decreasing the amount of water in soil. These factors do not play an important role during the short heavy rainfall season, but they can be critical for rainfall in the long period. On the other hand, artificial effects such as road cuts and construction activities like infrastructure and superstructure can be the cause of instability of soil masses. In this study, Landsat ETM + data for the years 2001 and 2002 were used to produce a 30-m resolution land cover map. Eight land cover types covering bulk of the study area were identified. After the classification process using maximum likelihood classifier, a thematic map was produced, including pasture (38 %), broadleaved forest (33 %), hazelnut fields (11 %), agricultural lands (8 %), coniferous trees (6 %), rocky areas (2 %), urban lands (1 %), and green tea lands (1 %).

Elevation

Elevation (i.e., height above the sea level) is known by its effects on biological and natural factors. An increase in elevation causes a corresponding decrease in temperature and rainfall, and these changes cause different plant types to grow. Vivas (1992) indicates that these conditions are likely to affect slope stability. Influence of elevation on landslide susceptibility is a subject open to argument, and this issue is yet to be clarified by the researchers. However, some researchers utilized the elevation data in the mapping of landslide susceptibility (e.g., Dai and Lee 2002; Gómez and Kavzoglu 2005). Due to the above considerations, the elevation data derived from the DEM of the study area were employed in landslide susceptibility modeling. Elevations ranging from 0 to 3,385 m were categorized by 500-m equal intervals. As a result, a thematic map with seven elevation classes was produced.

Aspect

Aspect is the orientation or direction of slope that is measured clockwise in degrees from 0° to 360°, where 0° is north-facing, 90° is east-facing, 180° is south-facing, and 270° is west-facing. Aspect associated parameters such as exposure to sunlight, drying winds, rainfall (degree of saturation), and discontinuities are important factors in triggering landslides (Dai et al. 2001). In the present work, the DEM image was used to calculate the aspect values for each pixel to construct the aspect image. Then, the image was reclassified into ten categories: flat (−1°), north (0°–22.5°, 337.5°–360°), northeast (22.5°–67.5°), east (67.5°–112.5°), southeast (112.5°–157.5°), south (157.5°–202.5°), southwest (202.5°–247.5°), west (247.5°–292.5°), northwest (292.5°–337.5°).

Drainage density

Drainage density is the total length of all streams and rivers in a drainage basin divided by the total area of the drainage basin. Drainage density provides an indirect measure of groundwater conditions having an important role in landslide activity. Sarkar and Kanungo (2004) state that there is an adverse relationship between landslides and drainage density. Considering the relationship between drainage density and landslide, it can be stated that as the drainage density increases, the landslide susceptibility increases. Drainage density is calculated from;

$$D_y = \sum L/A \tag{1}$$

where D_y is the drainage density, L is the stream length, and A is the catchment area. D_y was estimated for each catchment area, that is, drainage density value was constant for all pixels within the same catchment region. Drainage density map of the study area was produced from the DEM using an appropriate algorithm in ArcGIS software. The resulting map was reclassified into eight classes with equal intervals to be used in subsequent analyses.

Topographic wetness index

TWI was developed by Beven and Kirkby (1979) within the rainfall-runoff model TOPMODEL. At any point within a river basin, TWI is represented by a theoretical measure of the accumulation of flow. Soil moisture effect on slope material causes pore water pressures and decreases the soil strength, and thus, soil moisture directly influences slope instability, particularly for landslides. TWI is widely used in shallow landslide susceptibility mapping (Gokceoglu et al. 2005; Gómez and Kavzoglu 2005; Yilmaz 2009). In the estimation of wetness index, the sinks in the raster image are removed using a depressionless DEM algorithm. After the determination of multiple flow directions from the resulting DEM image, flow accumulation area (A_s) and tangent of slope (tan β) images are produced. TWI data of the study area were created using the equation given below,

$$\mathrm{TWI} = \mathrm{ln}(\mathrm{A_s}/\tan\beta) \tag{2}$$

where A_s is the specific catchment area and β is from the slope gradient. Topographic wetness index map, including values ranging from −4.46 to 16.06, was reclassified into ten classes with equal intervals of the TWI values.

Distance to road

Distance to road has a strong relation with landslide occurrence that can be the cause of cut slope creations through construction of roads that disturbs the natural topology and affects the stability of the slope. The existing roads built on sloping lands cause topographical changes under static load. The stability of a slope may change from stable to unstable during road constructions and vehicle movements (Collins 2008; Yalcin et al. 2011). These slope activities may occur as a result of cracks that lead to high water absorption of the soil and these negative influences, such as water saturation, can trigger landslides. This study also considers proximity to the roads for landslide occurrence. For this reason, distance to road map was created from an existing shapefile through a buffer analysis based on 25-m distance intervals from the central line of the roads.

Slope length

The slope length parameter has been considered in many GIS-based applications including landslides and soil erosions (Hickey 2000; Gómez and Kavzoglu 2005). Slope length can be defined as the distance along a slope subject to uninterrupted overland flow. It is an important factor in landslide activity since longer slope lengths increase the potential of erosive agents to transport materials downslope (Gómez and Kavzoglu 2005). Short slope lengths lead to limited flow velocity; therefore, soil masses cannot get enough flow energy to detach and transport materials over downslope (Chaplot and Le Bissonnais 2000). Slope lengths are computed on the horizontal and normal to the contours of the surface of the slope. Slope length is calculated by following formulation

(Liu et al. 2000; Conforti et al. 2011):

$$L = (\lambda/22.1)^m \tag{3}$$

where L is the slope length, λ is the slope length along the horizontal projection rather than along the sloping surface, and m is the relationship between the length and degree of slope, and it is defined as,

$$m = \beta(1+\beta) \tag{4}$$

where β is the ratio of rill erosion to interrill erosion. In the present study, the slope length map was derived by the DEM of the study area, and then it was divided into ten classes at 25-m equal intervals.

Landslide susceptibility mapping methods

In this study, landslide susceptibility maps were generated using GIS-based MCDA, SVR, and logistic regression methods. After applying the MCDA and SVR methods, logistic regression model was used as a benchmark method to compare and validate the performances in the determination of shallow landslide susceptibilities. The quality of the resulting thematic maps was tested using both accuracy measures and ROC curves.

GIS-based multi-criteria decision analysis

GIS-based MCDA is a process that transforms and combines geographical data and value judgments to obtain information for decision making (Malczewski 1999). Although several methods exist for estimation of decision criteria in the MCDA, the analytical hierarchy process (AHP) developed by Saaty (1980) is the most popular one. AHP is a flexible, yet structured methodology for analyzing and solving complex decision problems by structuring them into a hierarchical framework. It is employed for rating/ranking a set of alternatives or for the selection of the best in a set of alternatives. The ranking is carried out with respect to an overall goal, which is broken down into a set of criteria (objectives or attributes) (Boroushaki and Malczewski 2008). In other words, AHP is used to determine the weights of each criterion and analyze the relative importance of these criteria.

The first step of the AHP procedure is to decompose the decision problem into a hierarchy that consists of the most important elements of the decision problem. In developing a hierarchy, the top level is the ultimate goal of the decision at hand (Malczewski 1999). For spatial decision problems, decision elements are represented by a GIS database. In the second step, the input data are collected by pairwise comparison of decision elements, which is the basic measurement mode employed in the AHP procedure. Factor weights are obtained from the pairwise comparison matrix or ratio matrix undertaking eigenvalues and eigenvectors calculations. Pairwise comparison matrix is defined as follows:

$$A = \begin{pmatrix} a_{11} & a_{12} & \cdots & a_{1n} \\ a_{21} & a_{22} & \cdots & a_{2n} \\ \vdots & \vdots & \ddots & \vdots \\ a_{n1} & a_{n2} & \cdots & a_{nm} \end{pmatrix} = \begin{pmatrix} 1 & w_1/w_2 & \cdots & w_1/w_n \\ w_2/w_1 & 1 & \cdots & w_2/w_n \\ \vdots & \vdots & \ddots & \vdots \\ w_n/w_1 & w_n/w_2 & \cdots & 1 \end{pmatrix} \tag{5}$$

where A is the comparison matrix, which entry a_{ij} expresses how much the criteria x_i is preferred to criteria x_j. If all criteria are already known, each comparison value a_{ij} equals to w_i/w_j. In order to determine the relative weights, decision makers are asked to make pairwise comparison with values ranging from 1 to 9 (Table 1).

Criterion maps and their resulting weights can be used in weighted linear combination (WLC) function to aggregate criteria and produce a single score. WLC function is used to standardize the factor maps, ensuring that the sum of the set of factor weights is equal to 1. The overall scores are calculated for all criteria, and the criterion with the highest overall score is chosen. WLC method can be described by the following formula,

$$S = \sum_i w_i \mu_i \tag{6}$$

where S is the final score, w_i is the normalized weight of the criterion i, and μ_i is the criterion standardized score of the creation. Each factor map must be standardized or normalized to a same scale. The normalization process is identical to the process introduced by fuzzy logic, according to which a set of values expressed on a given scale is converted to another comparable set, expressed on a normalized scale (Melo et al. 2006). The fuzzy set theory introduced by Zadeh (1965) is, in short, the step following approximation between the precision of classical mathematics and the imprecision of the real world. The fuzzy set theory provides a rich mathematical basis for understanding decision problems and constructing decision rules in criteria evaluation and combination (Eastman 2003). In this theory, all factor layers are standardized to a continuous scale of suitability from 0 to 255 or from 0 to 1. Zero is assigned to the least vulnerable areas and 255 (or 1) to the most vulnerable areas, which is used to create thematic map layers. In this study, the "FUZZY" module of IDRISI was used for constructing fuzzy set membership functions.

Table 1 Scales for pairwise comparisons

Intensity of importance	Verbal judgment of preference
1	Equal importance
3	Moderate importance
5	Strong importance
7	Very strong importance
9	Extreme importance
2, 4, 6, 8	Intermediate values between adjacent scale values

Support vector machines

SVMs based on the statistical learning theory has been widely used as a data mining technique to solve many complex classification and regression problems (Brenning 2005; Kavzoglu and Colkesen 2009; Ballabio and Sterlacchini 2012). SVMs are originally developed as a binary classifier aiming to find a linear hyperplane that separates two classes optimally (Vapnik 1999). For binary classification problems, SVMs try to find a

separating hyperplane in the feature space such that the distance between the positive and negative samples is maximized for the linearly separable case (Fig. 3a). The hyperplane providing maximum margin between two classes is called optimum hyperplane and the points that constrain the width of the margin are called support vectors. In many classification and regression problems, it is difficult to separate data linearly (Fig. 3b). In such cases, the technique can be extended to allow for nonlinear decision surfaces (Cortes and Vapnik 1995). SVMs can handle data possessing of non-linear relationship using the kernel functions $(K(x_i, x) = \varphi(x_i).\varphi(x))$. As illustrated in Fig. 3b, these functions transform the original input space to a higher dimensional feature space where an optimal linear separating hyperplane is constructed.

Support vector regression with ε-intensive loss function (SVR) seeks an optimum hyperplane, from which the distance to all data points is minimum. When it is assumed that a training data set containing n number of samples is represented by $\{x_i, y_i\}$ $(i=1, \ldots, n)$ where x_i is the input and y_i is the output, the problem is to seek a function $f(x)$ that has at most ε deviation from the actually obtained target y_i for all training data and, at the same time, is as flat as possible (Smola and Scholkopf 2004). As it can be seen from Fig. 4, the hyperplane is defined as a linear function $f(x) = \langle w.x \rangle + b$, where x is a point lying on the hyperplane, parameter w determines the orientation of the hyperplane in space, and b is the bias that is the distance of hyperplane from the origin.

SVR performs linear regression in a high dimension feature space using ε-insensitive loss function and, at the same time, tries to reduce model complexity by minimizing $\|w\|^2$ (Cherkassky and Ma 2004). Thus, SVR is formulated as minimization of the following optimization problem,

$$\text{Minimize} \quad \tfrac{1}{2}\|w\|^2 + C\sum_{i=1}^{1}\xi_i + \xi_i^* \tag{7}$$

$$\text{subject to} \quad \left\{ \begin{array}{c} y_i - \langle w.x_i \rangle - b \le \varepsilon + \xi_i \\ \langle w.x_i \rangle + b - y_i \le \varepsilon + \xi_i^* \\ \xi_i, \xi_i^* \ge 0 \end{array} \right\} \tag{8}$$

where ξ_i and ξ_i^* $(i=1 \ldots n)$ are slack variables that measure the deviation of training samples outside ε-insensitive zone, and C is the regularization constant or penalty parameter that determines the trade-off between training error and model complexity. The SVR function that approximates the non-linear training data can be written as,

$$f(x) = (w.\varphi(x) + b) = \sum_{i=1}^{n}(a_i - a_i^*)K(x_i, x) + b \tag{9}$$

where α_i and α_i^* are Lagrange multipliers $\left(a_i \ge 0, a_i^* \le C\right)$.

The generalization performance of SVR depends on the setting of some parameters, namely C, ε, and kernel-related parameters. In

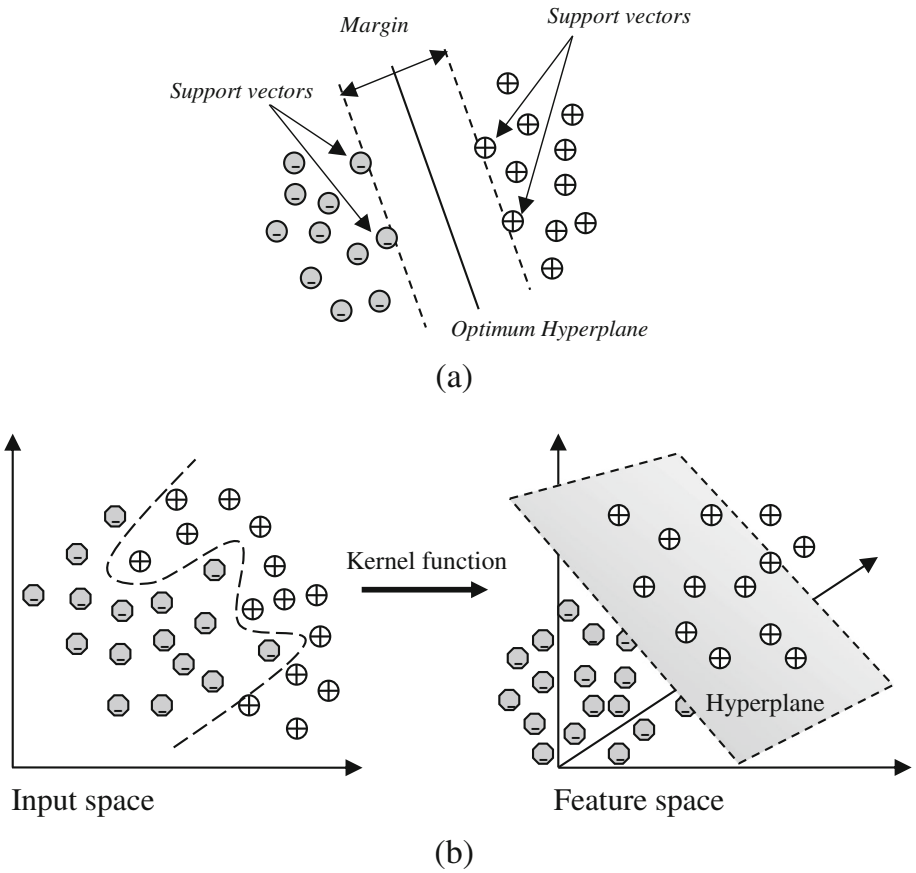

Fig. 3 Hyperplanes for **a** linearly separable data and **b** non-linear separable data

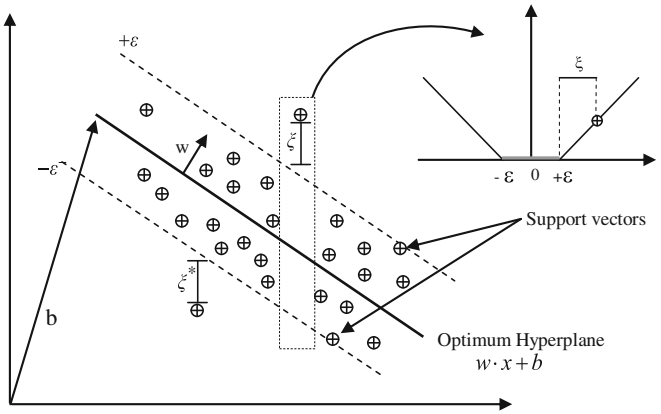

Fig. 4 The insensitive band for one dimensional linear regression problem

this study, radial basis function was chosen as the kernel function due to its robustness as reported by researchers (e.g., Cherkassky and Mulier 2007; Kavzoglu and Colkesen 2009).

Logistic regression model

Logistic regression (LR) model is measured with dichotomous variables such as 0 or 1, and it is determined from one or more independent factors (Menard 2001). The general purpose of the model is to determine the best fitting model to describe the relationship between the dependent variable (e.g., landslides) and set of independent parameters (e.g., slope, land cover, lithology). The advantage of the model is that the dependent variable can have only two values, an event occurring or not occurring, and that predicted values can be interpreted as probability since they are constrained to fall in the interval 0 and 1 (Dai and Lee 2002). LR model is based on the generalized linear model that can be calculated by the following equation:

$$P = \frac{1}{(1+e^{z})} \tag{10}$$

where P is the probability of an event. Z is a value from $-\infty$ to $+\infty$, defined by the following equation;

$$Z = B_0 + B_1X_1 + B_2X_2 + \ldots + B_nX_n \tag{11}$$

B_0 is the intercept of model, n is the number of independent variables, and B_1, B_2, …, B_n are coefficients, which measure the contribution of independent variables (X_1, X_2, …, X_n) (Ayalew and Yamagishi 2005; Akgun 2012). In the logistic regression model, the dependent variable can be expressed as,

$$\text{Logit}(p) = \ln(p/(1-p)) = 1/1 + e^{-B_0+B_1X_1+B_2X_2+\cdots+B_nX_n} \tag{12}$$

where p is the probability that the dependent variable has values of only 0 and 1 and $p/(1-p)$ is the so-called odds or likelihood ratio. Probabilities vary between 0 and 1. As a probability gets closer to 1, the numerator of the odds becomes larger relative to the denominator, and the odds become an increasingly large number. On the contrary, if a probability gets closer to 0, the numerator of the odds becomes smaller relative to the denominator (Ayalew and Yamagishi 2005).

Results and discussions

The effectiveness of MCDA and SVR methods was evaluated for landslide susceptibility mapping problem considered in this study. Performances of the methods were compared with that of LR model that is widely used in the literature. In order to apply these methods, training and test data sets, including landslide and non-landslide zones, were created using a ground reference map. Image layers representing the landslide-related parameters considered in this study were stacked to compose a multi-layer image. The ground reference map and the multi-layer image were used to create the training and testing data sets using a random sampling strategy. The data sets were created with equal numbers of samples for each class (i.e., landslide and non-landslide). With the above considerations, 4,000 pixels for training and 6,000 pixels for

Table 2 Fuzzy membership functions used for landslide factors

Factors	Fuzzy sets Function type	Function form	Fuzzy numbers
Lithology	User-defined	$f_{(\text{lithology})}$[a]	–
Slope	Sigmoidal	Monotonically increasing	a,b,c=5°, d=27°
TWI	Sigmoidal	Monotonically increasing	a,b,c=−4.49, d=16.06
Land cover	User-defined	$f_{(\text{land cover})}$[b]	–
Drainage density	Sigmoidal	Monotonically increasing	a,b,c=0, d=0.0006
Aspect	User-defined	$f_{(\text{aspect})}$[c]	–
Slope length	Sigmoidal	Monotonically decreasing	a,b,c=0 m, d=1,000 m
Elevation	Sigmoidal	Monotonically decreasing	a,b,c=0 m, d=2,500 m
Distance to road	Sigmoidal	Symmetric	a=0, b=25, c=75, d=125 m

[a] $f_{(\text{lithology})}$=(0.4/1, 0.3/2, 0.5/3, 0.8/4, 0.1/5, 0.1/6, 0.1/7, 0.6/8, 1/9, 0.7/10, 0.8/11, 0.8/12, 0.5/13)

[b] $f_{(\text{land cover})}$=(1/1, 0.4/2, 0.3/3, 0.2/4, 0.8/5, 0/6, 0.7/7, 0/8)

[c] $f_{(\text{aspect})}$=(0.2/1, 0.5/2, 1/3, 0.5/4, 0.2/5, 0.8/6, 1/7, 0.8/8, 0.1/9)

testing were selected for further processes. It should be noted that the same training and test data sets were employed in the application of all methods considered in this study.

A variety of performance measures were discussed in the literature to analyze the thematic map accuracy (Foody 2004). However, individual and overall accuracy measures derived from the error matrix have been the most popular ones. On the other hand, several statistical tests including F-measure, mean squared error, and ROC statistics have been suggested to compare performances of the methods (De Leeuw et al. 2006; Ferri et al. 2009). In this study, in addition to user's and overall accuracies derived from contingency matrices, success rate curve and ROC statistics, which show goodness of fit, were used to compare the performances of the landslide susceptibility methods.

Multi-criteria decision analysis model

Since the input layers representing landslide-related parameters or factors were at different scales or intervals, they were standardized using AHP method, as described above. Landslide factor maps were standardized based on fuzzy membership function using "FUZZY" module of Idrisi Taiga software. In the standardization of factor maps, sigmoidal fuzzy membership functions and user-defined functions were used for each factor (Table 2). A monotonically increasing sigmoidal fuzzy membership function was used for slope, TWI, and drainage density images, while a monotonically decreasing sigmoidal fuzzy membership function was used for slope length and elevation images. On the other hand, user-defined membership functions were applied for lithology, land cover, and aspect images.

Calculation of the factor weights has a crucial role in the production of landslide susceptibility maps when applying the MCDA technique. The eigenvector method based on pairwise comparison was employed for this purpose, in that each factor was ranked considering its importance by scale ranging from 1 to 9. After the pairwise comparison matrix was formed, weights of the factors were calculated (Table 3). It was seen that the highest weight was assigned to the lithology map, which is considered as an expected result considering the previous studies in the field (e.g., Yalcin et al. 2011; Akgun 2012). Slope, TWI, and land cover factors were also found effective (i.e., primary factors). The others (i.e., aspect, slope length, drainage density, elevation, and distance to road) were identified as less important or secondary parameters.

In AHP method, consistency ratio (CR) is used to indicate the probability that the matrix judgments were randomly generated. CR value of 0.1 or less is a reasonable level of consistency (Malczewski 1999). If the CR value is greater than this level, inconsistency of judgments within that matrix occurs, and the evaluation process should revise the original values in the pairwise comparison matrix. In this study, the CR value for the pairwise comparison matrix was estimated as 0.06, confirming a valid consistency.

Each evaluated factor was calculated using WLC method available in MCE module of Idrisi Taiga software. The weights from pairwise comparison matrix were multiplied by the factor maps, and all weighted factor maps were then aggregated. At this point, the resulting map was reclassified into several meaningful susceptibility classes for presentation and evaluation purposes. In the literature, several mathematical or experimental approaches including natural breaks, standard deviations, equal interval, and expert-based classifiers have been suggested for this purpose (Guzzetti et al. 1999; Ayalew et al. 2004; Suzen and Doyuran 2004; Akgun 2012). An expert-

Table 3 The pairwise comparison matrix and factor weights

	Lithology	Slope	Land cover	TWI	Aspect	Slope length	Drainage density	Elevation	Distance to road	Weights
Lithology	1									0.3074
Slope	1	1								0.2900
Land cover	0.20	0.20	1							0.1259
TWI	0.20	0.20	0.50	1						0.0920
Aspect	0.143	0.25	0.50	0.50	1					0.0567
Slope length	0.143	0.143	0.20	0.333	1	1				0.0481
Drainage density	0.143	0.143	0.20	0.25	0.50	0.50	1			0.0355
Elevation	0.143	0.143	0.167	0.20	0.333	0.333	0.50	1		0.0265
Distance to road	0.125	0.125	0.167	0.167	0.25	0.25	0.25	0.333	1	0.0181

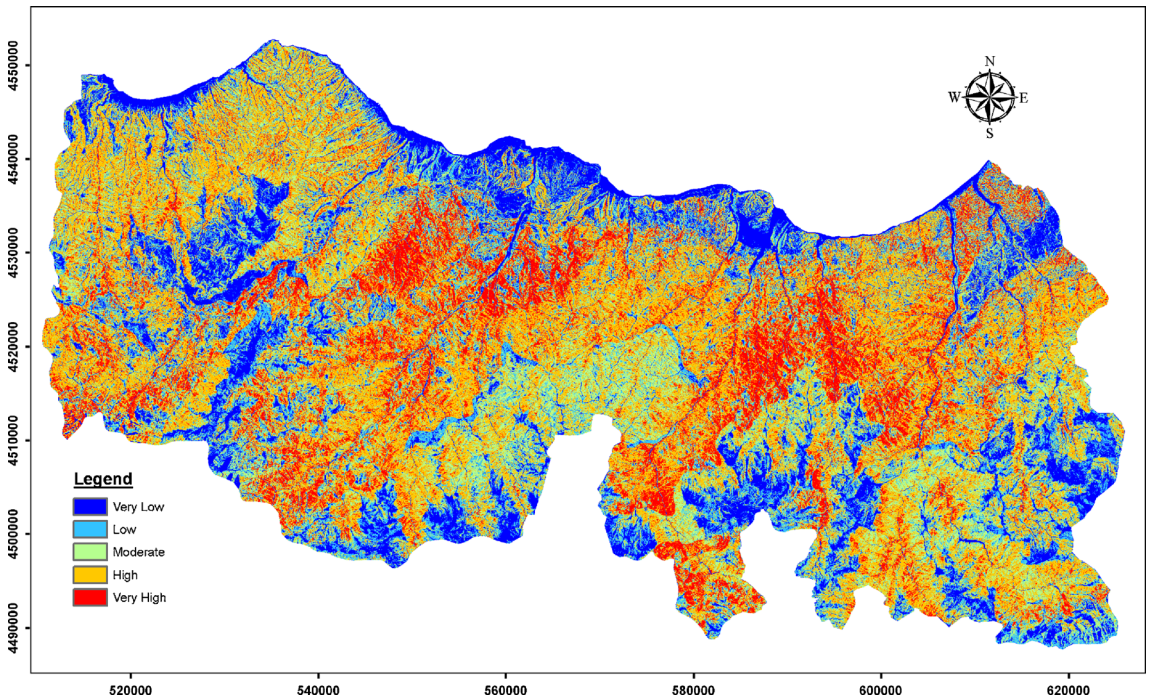

Fig. 5 Landslide susceptibility map produced by GIS-based MCDA method

based classification or density slicing was used to define class intervals in this study. All landslide susceptibility maps were reclassified into five susceptibility levels as: very low, low, moderate, high, and very high (Fig. 5). It was observed that high landslide-susceptibility zones were generally situated in the central part of the study area. These zones were mainly located on the areas with high slope and sensitive lithological units (e.g., Cru1, Cru2, and Cru3). On the other hand, the north (i.e., coastline) and south sides of the study area were generally covered by low susceptibility zones.

Support vector regression model

The SVR model was utilized together with the radial basis function kernel to produce a landslide susceptibility map of the study area. Meta-parameters of C, ε, and γ (kernel width) were selected after a

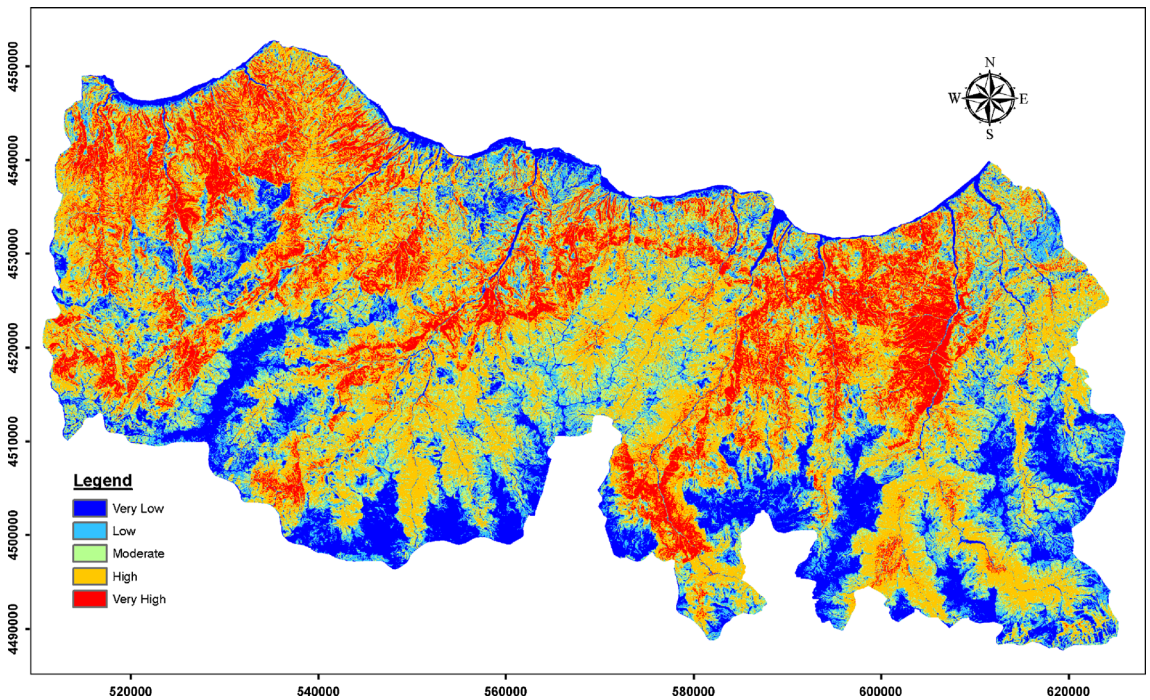

Fig. 6 Landslide susceptibility map produced by SVR model

Table 4 Logistic regression coefficients and Wald statistics

Variable	β	SE	Wald	Significance
Slope	1.094	0.047	532.559	0.000
Drainage Density	0.664	0.033	412.072	0.000
Elevation	−0.550	0.060	85.468	0.000
TWI	−0.329	0.063	27.496	0.000
Slope length	0.238	0.110	532.559	0.030
Land cover	−0.076	0.026	8.900	0.003
Distance to road	−0.046	0.042	1.193	0.275
Lithology				
Alv	−4.406	0.390	127.734	0.000
Pl	3.560	0.422	71.324	0.000
Y_3	−14.744	0.000	0.000	0.000
Ev	6.342	0.322	388.681	0.000
Y_2	2.515	0.326	59.324	0.000
Cru5a	4.199	0.323	169.039	0.000
Cru5b	−17.267	8,452.354	0.000	0.998
Cru4b	10.204	0.455	503.235	0.000
Cru3	8.980	0.334	724.465	0.000
Cru2	10.647	0.540	389.281	0.000
Cru1	10.733	0.435	607.916	0.000
JCr	−0.242	0.346	0.488	0.485
Jlh	−0.001	0.000	0.000	0.000
Aspect				
Flat	−2.652	0.678	15.279	0.000
0–22.5	0.791	0.334	5.609	0.018
22.5–67.5	1.112	0.268	17.199	0.000
67.5–112.5	1.261	0.263	22.941	0.000
112.5–157.5	1.063	0.265	16.123	0.000
157.5–202.5	1.289	0.279	21.295	0.000
202.5–247.5	1.272	0.293	18.905	0.000
247.5–292.5	1.544	0.274	31.816	0.000
292.5–337.5	0.908	0.262	12.026	0.001
337.5–360	−0.001	0.000	0.000	0.000

cross-validation stage. As a result, optimum values of ε, C, and γ were determined as 0.001, 100, and 0.1, respectively. Root mean square error was calculated as 0.30 when the trained SVR model was tested on the test data set. The model was then applied to the multi-layer image consisting of nine landslide parameters to estimate the susceptibilities of the pixel in the image. Resulting susceptibility map was reclassified to show five susceptibility levels using expert-based classification approach (Fig. 6). In contrast to the MCDA procedure (Fig. 5), the north-west side of Trabzon province was mainly classified as very high and high susceptible zones. Also, a large number of high susceptible zones were located in the north-east of the study area. These zones are mostly located on the lithological units of Ev, Cru2, and Cru3. Moderate susceptible zones were usually located in the east and central parts of the study area. Lastly, the south and south-east parts of the study area were largely described as low susceptibility.

Logistic regression model

LR model was employed as a benchmark method to estimate the probabilities for landslide susceptibility map. In performing susceptibility analysis, the independent variables were lithology, slope, land cover, TWI, slope length, road to distance, elevation, aspect, and drainage density, whilst the dependent variable was landslide samples in the inventory map. It should be noted that the ground reference map comprising 147 landslide fields (12,029

Table 5 The multicollinearity analysis for variables

Variable	TOL	VIF
Slope	0.465	2.152
Drainage density	0.584	1.713
Elevation	0.467	2.141
TWI	0.737	1.358
Slope length	0.529	1.890
Land cover	0.857	1.167
Distance to road	0.907	1.103
Lithology	0.634	1.576
Aspect	0.882	1.134

pixels) and 70 non-landslide fields (6,280 pixels) were used to produce a dependent variable. The spatial relationship between landslide occurrence and landslide-related parameters was determined through the coefficients of the logistic regression model using SPSS software (Table 4). While the positive values of the logistic regression coefficient imply that the occurrence of landslides is positively related (i.e., the independent variable increases the probability of a landslide), negative values of the coefficients have a negative relationship with the landslide occurrence. The Wald test was employed to assess the statistical significance of the coefficients (β) representing individual variables. The Wald statistical values increase with significance of β coefficients. Among lithological units, Cru3, Cru1, and Cru4b are the main landslides conditioning factors, respectively. When all variables are considered, it can be easily noticed that the slope angle is the most effective factor as expected. On the other hand, distance to road variable is found the least effective variable among the others.

When more than two variables are involved, this is often called as multicollinearity, and model fitting with logistic regression is sensitive to collinearities among the independent variables (Hosmer and Lemeshow 1989). Tolerance (TOL) and the variance inflation factor (VIF) are two important indices to assess the multicollinearity among the variables. A TOL value less than 0.2 is an indicator for multicollinearity, and serious multicollinearity occurs between independent variables when the TOL values are smaller than 0.1 (Menard 2001). If VIF value exceeds 10, it is often regarded as an indication for multicollinearity. The TOL and VIF values in this study are estimated and shown in Table 5, indicating that there is no multicolinearity between any of the variables considered in this study.

Landslide susceptibility map generated by the logistic regression method was also reclassified into five susceptibility classes using expert-based classification approach (Fig. 7). The north of the study area was generally identified as highly susceptible to landslides, whilst the south was determined as having low susceptibility to landslides. High and very high susceptibility regions were mostly located on lithological units of Ev, Cru2, and Cru4b.

Analysis of the results

In order to determine the accuracies of the landslide susceptibility maps produced by the three methods, confusion matrices were calculated using the test data set (Table 6). It should be noted that lands classified as very high, high, and moderate were considered as landslide zones, and the rest (i.e., low and very low) were considered as non-landslide zones in accuracy assessment stage. The GIS-based MCDA, SVR, and LR methods resulted in classifications with overall accuracies of 77.49 %, 75.12 %, and 69.29 %, respectively. That is, the GIS-based MCDA method was superior to the other methods with slight difference with the SVR method. The

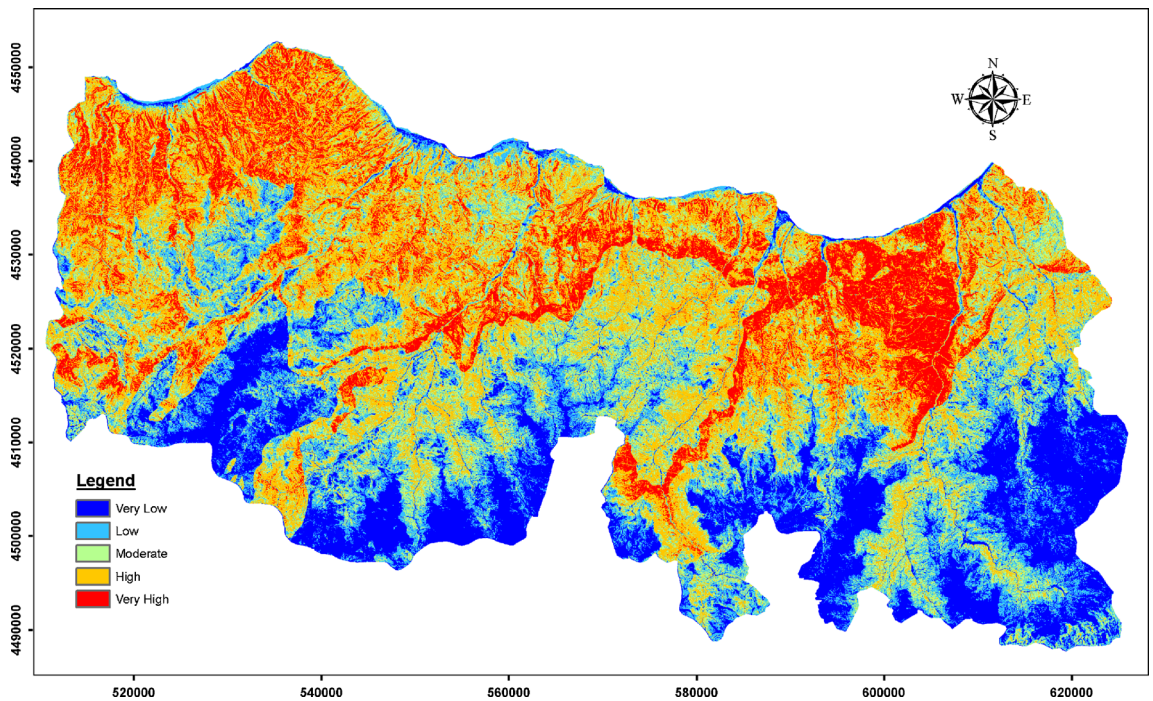

Fig. 7 Landslide susceptibility map produced by logistic regression

Table 6 Confusion matrices estimated for MCDA, SVR, and LR

		Landslide	Non-landslide	User's accuracy (%)
MCDA	Landslide	8,514	3,515	70.78
	Non-landslide	607	5,673	90.33
	Overall accuracy=77.49 %			
SVR	Landslide	8,631	3,398	71.75
	Non-landslide	1,158	5,122	81.56
	Overall accuracy=75.12 %			
LR	Landslide	7,773	4,256	64.62
	Non-landslide	1,345	4,935	78.58
	Overall accuracy=69.41 %			

LR method produced the lowest performance. Another accuracy measure applied to the test data set was the user's accuracy showing the probability that pixels classified on the image actually represents that category on the ground. This accuracy measure was used to estimate individual accuracies of the classes (i.e., landslide and non-landslide pixels), and the results are given in Table 6. It can be seen from the table that the highest user's accuracies were produced by the GIS-based MCDA method as 90.33 % for non-landslide pixels and by the SVR method as 71.75 % for landslide pixels present in the test data set. On the other hand, the lowest user's accuracies for landslide (64.62 %) and non-landslide (78.58 %) pixels were both obtained by the LR method. When the individual accuracies of the methods were considered, the GIS-based MCDA method can be declared as the "best" method generating lower misclassification rates.

In order to determine the statistical reliability of the results, the area under the ROC curve, or simply AUC, and success rate curve were employed. The AUC is a good indicator to evaluate the prediction performance of the model, and the largest AUC, varying from 0.5 to 1.0, is the most ideal model (Yesilnacar and Topal 2005; Yilmaz 2010). AUC values between 0.7 and 0.9 indicate reasonable discrimination ability. Additionally, AUC values higher than 0.9 show typical of highly accurate classification models (Swets 1988). The ROC curves and calculated AUC values for the MCDA, SVR, and LR methods are shown in Fig. 8. AUC values of the MCDA, SVR, and LR models were calculated as 0.9384, 0.9321, and 0.9108, respectively, indicating acceptable level of performance.

In order to obtain the success rate curve for each susceptibility map, the calculated prediction values of all pixels in the susceptibility images were sorted in descending order. Values were then categorized into 100 classes with 1 % cumulative intervals in ArcGIS 10. These maps were overlaid with the landslide inventory map of the study area. Thus, the success rate curves of the three methods were created from the cross-table values (Fig. 9). The

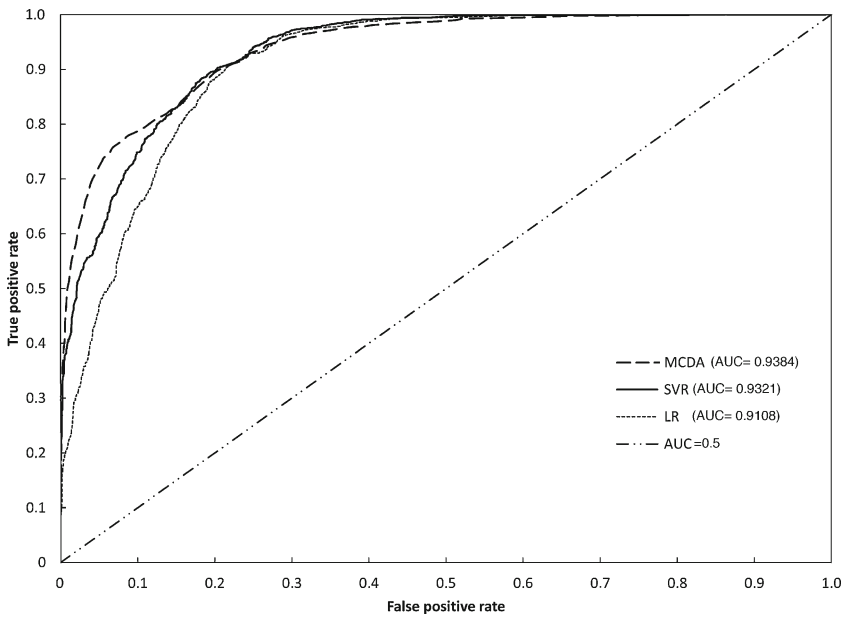

Fig. 8 ROC statistics for the methods used in landslide susceptibility

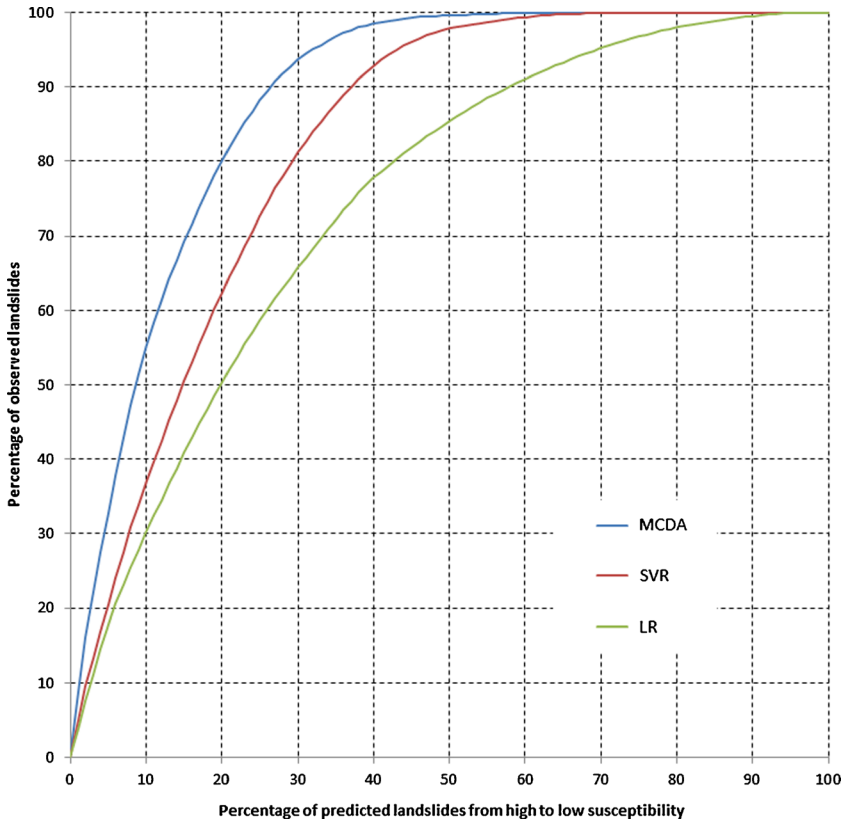

Fig. 9 Success rate curves of landslide susceptibility values calculated from MCDA, SVR, and LR methods

success rate analysis reveals that 10 % of the study area where susceptibility rate had a higher rank could explain approximately 55 % of observed landslides for MCDA, 37 % for SVR, and 30 % for LR. Similarly, 50 % of the study area could explain about 99 % of observed landslides for MCDA, 97 % for SVR, and 85 % for LR (Fig. 9).

Conclusions

Identification of landslide-prone regions and determining their locations according to given susceptibility levels play an important role for the success of planning activities. Many methods have been suggested in the literature to produce landslide susceptibility maps. In this study, effectiveness of the GIS-based MCDA and SVR methods were assessed in the determination of shallow landslide susceptibility map of Trabzon province in NE Turkey. Performances of the methods were compared with that of widely used logistic regression model. These methods were employed using lithology, slope, land cover, aspect, topographic wetness index, drainage density, slope length, elevation, and distance to road factors.

In the analysis of logistic regression results, the Wald statistics was applied to analyze the statistical significance of the coefficients and found that lithology and slope layers were the most effective factors leading to landslide occurrence in the study area. For multicolinearity testing, the TOL and VIF values were estimated, and it was found that there was no multicolinearity between any of the variables considered. When the logistic regression model was applied to whole image, the north of the study area was generally identified as highly susceptible to landslides that are mainly located on lithological units of Ev, Cru2, and Cru4b. On the other hand, the MCDA method indicated that high landslide susceptibility zones were generally situated in the central part of the study area that are mainly located on the lithological units of Cru1, Cru2, and Cru3. Conversely, the north-west side of Trabzon province was mainly classified as very high and high susceptible zones by the SVR method. These zones were mostly located on the lithological units of Ev, Cru2, and Cru3.

Accuracy assessment results showed that the MCDA and SVR methods outperformed logistic regression method by about 8 % in terms of overall accuracy considering ground reference map. On the other hand, the area under the ROC curves (AUC) and success rate curves were estimated to test the statistical reliability of the results. Considering both statistics, all methods generated acceptable results, and the GIS-based MCDA method produced slightly better results than the SVM method.

Compared with the logistic regression model, the GIS-based MCDA and SVR methods had several advantages, including handling complex and non-linear data sets. Besides these important advantages, these sophisticated methods have several drawbacks. The main difficulty in the use of the MCDA is the determination of optimal values of the weights assigned for each parameter pair, whereas the selection of kernel parameters and determination of their optimal values are crucial for the success of the SVR method. Although the logistic regression is a simple and widely used method, it was found inferior in shallow landslide susceptibility mapping considered in this study. To sum up, the GIS-based MCDA and SVR methods producing similar results were found effective in the

modeling of shallow landslide susceptibility in spite of difficulty or expertise required in their use.

References

Akgun A (2012) A comparison of landslide susceptibility maps produced by logistic regression, multi-criteria decision, and likelihood ratio methods: a case study at Izmir, Turkey. Landslides 9(1):93–106

Armas I (2011) An analytic multicriteria hierarchical approach to assess landslide vulnerability. Case study: Cornu village, Subcarpathian Prahova Valley/Romania. Z Geomorphol 55(2):209–229

Ayalew L, Yamagishi H (2005) The application of GIS-based logistic regression for landslide susceptibility mapping in the Kakuda-Yahiko Mountains, Central Japan. Geomorphology 65(1–2):15–31

Ayalew L, Yamagishi H, Ugawa N (2004) Landslide susceptibility mapping using GIS-based weighted linear combination, the case in Tsugawa area of Agano River, Niigata Prefecture, Japan. Landslides 1(1):73–81

Ayalew L, Yamagishi H, Marui H, Kanno T (2005) Landslides in Sado Island of Japan: part II. GIS-based susceptibility mapping with comparisons of results from two methods and verifications. Eng Geol 81(4):432–445

Bai SB, Lu GN, Wang JA, Zhou PG, Ding LA (2011) GIS-based rare events logistic regression for landslide-susceptibility mapping of Lianyungang, China. Environ Earth Sci 62(1):139–149

Ballabio C, Sterlacchini S (2012) Support Vector machines for landslide susceptibility mapping: the Staffora River Basin Case Study, Italy. Math Geosci 44(1):47–70

Bayrak T, Ulukavak M (2009) Trabzon heyelanları. Harita Teknolojileri Elektronik Dergisi 1(2):20–30 (in Turkish)

Begueria S (2006) Changes in land cover and shallow landslide activity: a case study in the Spanish Pyrenees. Geomorphology 74(1–4):196–206

Beven KJ, Kirkby MJ (1979) A physically based, variable contributing area model of basin hydrology. Hydrol Sci Bull 24(1):43–69

Boroushaki S, Malczewski J (2008) Implementing an extension of the analytical hierarchy process using ordered weighted averaging operators with fuzzy quantifiers in ArcGIS. Comput Geosci 34(4):399–410

Brenning A (2005) Spatial prediction models for landslide hazards: review, comparison and evaluation. Nat Hazard Earth Sys 5(6):853–862

Castellanos Abella EA, Van Westen CJ (2007) Generation of a landslide risk index map for Cuba using spatial multi-criteria evaluation. Landslides 4(4):311–325

Chaplot V, Le Bissonnais Y (2000) Field measurements of interrill erosion under different slopes and plot sizes. Earth Surf Proc Land 25(2):145–153

Cherkassky V, Ma YQ (2004) Practical selection of SVM parameters and noise estimation for SVM regression. Neural Netw 17(1):113–126

Cherkassky V, Mulier F (2007) Learning from data: concepts, theory and methods, 2nd edn. John Wiley & Sons, New Jersey

Collins TK (2008) Debris flows caused by failure of fill slopes: early detection, warning, and loss prevention. Landslides 5(1):107–120

Conforti M, Aucelli PPC, Robustelli G, Scarciglia F (2011) Geomorphology and GIS analysis for mapping gully erosion susceptibility in the Turbolo stream catchment (Northern Calabria, Italy). Nat Hazards 56(3):881–898

Cortes C, Vapnik V (1995) Support-vector networks. Mach Learn 20(3):273–297

Dai FC, Lee CF (2002) Landslide characteristics and, slope instability modeling using GIS, Lantau Island, Hong Kong. Geomorphology 42(3–4):213–228

Dai FC, Lee CF, Li J, Xu ZW (2001) Assessment of landslide susceptibility on the natural terrain of Lantau Island, Hong Kong. Environ Geol 40(3):381–391

De Leeuw J, Jia H, Yang L, Liu X, Schmidt K, Skidmore AK (2006) Comparing accuracy assessments to infer superiority of image classification methods. Int J Remote Sens 27(1):223–232

Devkota KC, Regmi AD, Pourghasemi HR, Yoshida K, Pradhan B, Ryu IC, Dhital MR, Althuwaynee OF (2013) Landslide susceptibility mapping using certainty factor, index of entropy and logistic regression models in GIS and their comparison at Mugling-Narayanghat road section in Nepal Himalaya. Nat Hazards 65(1):135–165

Eastman R (2003) Idrisi Kilimanjaro Manual and Tutorial. Clark Labs, Clark University, Worchester

Ergünay O (2007) Türkiye'nin afet profili. TMMOB Afet Sempozyumu, Ankara, pp 42–45 (in Turkish)

Ferri C, Hernandez-Orallo J, Modroiu R (2009) An experimental comparison of performance measures for classification. Pattern Recogn Lett 30(1):27–38

Foody GM (2004) Thematic map comparison: evaluating the statistical significance of differences in classification accuracy. Photogramm Eng Rem S 70(5):627–633

Fu WJ, He YR (2010) Landslide susceptibility evaluation based on fuzzy support vector machine. Sixth Int Symp Digit Earth Data Process Appl 7841. doi:10.1117/12.873267

Gokceoglu C, Sonmez H, Nefeslioglu HA, Duman TY, Can T (2005) The 17 March 2005 Kuzulu landslide (Sivas, Turkey) and landslide-susceptibility map of its near vicinity. Eng Geol 81(1):65–83

Gómez H, Kavzoglu T (2005) Assessment of shallow landslide susceptibility using artificial neural networks in Jabonosa River Basin, Venezuela. Eng Geol 78(1–2):11–27

Guzzetti F, Carrara A, Cardinali M, Reichenbach P (1999) Landslide hazard evaluation: a review of current techniques and their application in a multi-scale study, Central Italy. Geomorphology 31(1–4):181–216

Hickey R (2000) Slope angle and slope length solutions for GIS. Cartography 29(1):1–8

Hosmer DW, Lemeshow S (1989) Applied regression analysis. John Wiley and Sons, New York

Kavzoglu T, Colkesen I (2009) A kernel functions analysis for support vector machines for land cover classification. Int J Appl Earth Obs 11(5):352–359

Liu BY, Nearing MA, Shi PJ, Jia ZW (2000) Slope length effects on soil loss for steep slopes. Soil Sci Soc Am J 64(5):1759–1763

Malczewski J (1999) GIS and multicriteria decision analysis. John Wiley and Sons, Toronto

Melo ALO, Calijuri ML, Duarte ICD, Azevedo RF, Lorentz JF (2006) Strategic decision analysis for selection of landfill sites. J Surv Eng-Asce 132(2):83–92

Menard S (2001) Applied logistic regression analysis, 2nd edn. Sage Publication, Thousand Oaks, California

Nandi A, Shakoor A (2010) A GIS-based landslide susceptibility evaluation using bivariate and multivariate statistical analyses. Eng Geol 110(1–2):11–20

Neuhauser B, Damm B, Terhorst B (2012) GIS-based assessment of landslide susceptibility on the base of the weights-of-evidence model. Landslides 9(4):511–528

Pradhan B (2013) A comparative study on the predictive ability of the decision tree, support vector machine and neuro-fuzzy models in landslide susceptibility mapping using GIS. Comput Geosci 51(0):350–365

Pradhan B, Lee S (2010) Landslide susceptibility assessment and factor effect analysis: backpropagation artificial neural networks and their comparison with frequency ratio and bivariate logistic regression modelling. Environ Modell Softw 25(6):747–759

Restrepo C, Vitousek P, Neville P (2003) Landslides significantly alter land cover and the distribution of biomass: an example from the Ninole ridges of Hawai'i. Plant Ecol 166(1):131–143

Roy B (1996) Multicriteria methodology for decision aiding. Kluwer Academic Publishers, Dordrecht

Saaty TL (1980) The analytic hierarchy process: planning, priority setting. Resource allocation. McGraw-Hill, New York

Santacana N, Baeza B, Corominas J, De Paz A, Marturia J (2003) A GIS-based multivariate statistical analysis for shallow landslide susceptibility mapping in La Pobla de Lillet area (Eastern Pyrenees, Spain). Nat Hazards 30(3):281–295

Sarkar S, Kanungo DP (2004) An integrated approach for landslide susceptibility mapping using remote sensing and GIS. Photogramm Eng Rem S 70(5):617–625

Segoni S, Rossi G, Catani F (2012) Improving basin-scale shallow landslides modelling using reliable soil thickness maps. Nat Hazards 61:85–101

Smola AJ, Scholkopf B (2004) A tutorial on support vector regression. Stat Comput 14(3):199–222

Suzen ML, Doyuran V (2004) Data driven bivariate landslide susceptibility assessment using geographical information systems: a method and application to Asarsuyu catchment, Turkey. Eng Geol 71(3–4):303–321

Swets JA (1988) Measuring the accuracy of diagnostic systems. Science 240(4857):1285–1293

Vapnik VN (1999) The nature of statistical learning yheory, 2nd edn. Springer, New York

Varnes DJ (1978) Slope movement types and processes. In: Schuster RL, Krizek RJ (eds) Landslides analysis and control. National Academy of Sciences, New York, pp 12–33

Vivas L (1992) Los Andes Venezolanos. Academia Nacional de la Historia, Caracas

Wang WD, Xie CM, Du XG (2009) Landslides susceptibility mapping based on geographical information system, GuiZhou, south-west China. Environ Geol 58(1):33–43

Yalcin A (2011) A geotechnical study on the landslides in the Trabzon Province, NE, Turkey. Appl Clay Sci 52(1–2):11–19

Yalcin A, Reis S, Aydinoglu AC, Yomralioglu T (2011) A GIS-based comparative study of frequency ratio, analytical hierarchy process, bivariate statistics and logistics

regression methods for landslide susceptibility mapping in Trabzon, NE Turkey. Catena 85(3):274–287
Yao X, Tham LG, Dai FC (2008) Landslide susceptibility mapping based on support vector machine: a case study on natural slopes of Hong Kong, China. Geomorphology 101(4):572–582
Yesilnacar E, Topal T (2005) Landslide susceptibility mapping: a comparison of logistic regression and neural networks methods in a medium scale study, Hendek region (Turkey). Eng Geol 79(3–4):251–266
Yilmaz I (2009) Landslide susceptibility mapping using frequency ratio, logistic regression, artificial neural networks and their comparison: a case study from Kat landslides (Tokat-Turkey). Comput Geosci 35(6):1125–1138
Yilmaz I (2010) Comparison of landslide susceptibility mapping methodologies for Koyulhisar, Turkey: conditional probability, logistic regression, artificial neural networks, and support vector machine. Environ Earth Sci 61(4):821–836
Zadeh LA (1965) Fuzzy sets. Inform Control 8(3):338–353

T. Kavzoglu (✉) · E. K. Sahin · I. Colkesen
Department of Geodetic and Photogrammetric Engineering,
Gebze Institute of Technology,
Cayirova Campus, 41400, Gebze-Kocaeli, Turkey
e-mail: kavzoglu@gyte.edu.tr